JACC: BASIC TO TRANSLATIONAL SCIENCE VOL. 4, NO. 1, 2019

PRECLINICAL RESEARCH

miR-29b Mediates the Chronic Inflammatory Response in Radiotherapy-Induced Vascular Disease

Suzanne M. Eken, MD, PhD,[a] Tinna Christersdottir, MD,[b] Greg Winski, MD,[a] Traimate Sangsuwan, MSc,[c] Hong Jin, MD, PhD,[a] Ekaterina Chernogubova, PhD,[a] John Pirault, PhD,[d] Changyan Sun, MSc,[a] Nancy Simon, MSc,[a] Hanna Winter, MSc,[e,f] Alexandra Backlund, PhD,[a] Siamak Haghdoost, PhD,[c,g] Göran K. Hansson, MD, PhD,[a] Martin Halle, MD, PhD,[b,h,*] Lars Maegdefessel, MD, PhD[a,e,f,*]

VISUAL ABSTRACT

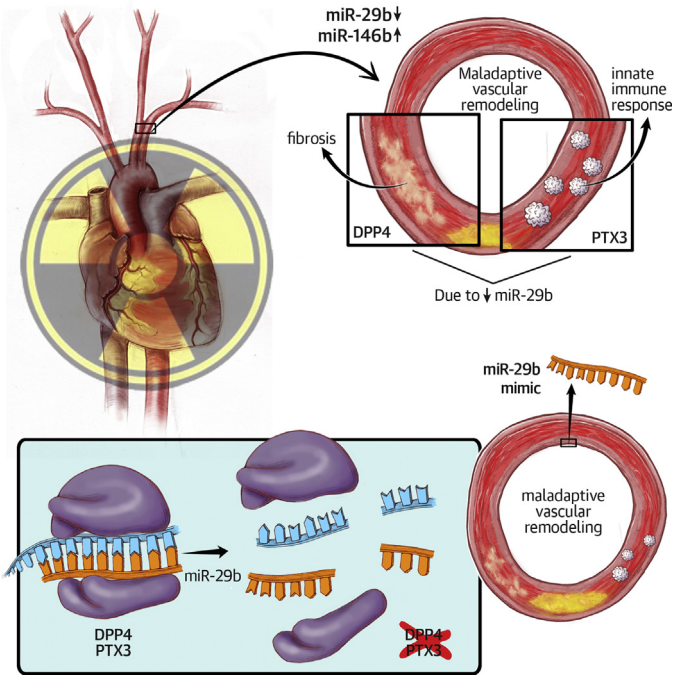

Eken, S.M. et al. J Am Coll Cardiol Basic Trans Science. 2019;4(1):72–82.

HIGHLIGHTS

- **Radiotherapy is a powerful treatment strategy in patients with oncological diseases.**
- **Radiation-induced vasculopathy can dose dependently increase the risk of ischemic cardiovascular diseases (e.g., myocardial infarction, heart failure, stroke).**
- **The microRNA miR-29b is repressed in radiation-induced vasculopathy (human irradiated vs. nonirradiated tissue specimen, as well as in murine and cell culture models of irradiation).**
- **Pentraxin-3 and dipeptidyl-peptidase 4 are the main downstream effectors of miR-29b in radiation-induced vasculopathy.**
- **miR-29b mimics were able to limit pentraxin-3 and dipeptidyl-peptidase 4 levels in the irradiated vasculature (murine model) and to constrain the burden of vascular inflammation.**

From the [a]Cardiovascular Medicine Unit, Department of Medicine, Solna, Karolinska Institute, Stockholm, Sweden; [b]Department of Molecular Medicine and Surgery, Karolinska Institute, Stockholm, Sweden; [c]Department of Molecular Biosciences, Wenner-Gren Institute, Stockholm University, Stockholm, Sweden; [d]INSERM UMR_S1116, Université de Lorraine, Vandoeuvre-lès-Nancy, France; [e]Technical University Munich, Department of Vascular and Endovascular Surgery, Munich, Germany; [f]German Center for Cardiovascular Research (DZHK) partner site Munich, Munich, Germany; [g]University of Caen Normandie, LARIA-CIMAP, Caen, France; and the [h]Department of Reconstructive Plastic Surgery, Karolinska University Hospital, Stockholm, Sweden. *Drs. Halle and Maegdefessel contributed equally to this work and are joint senior authors. The study was supported through funding from Radiumhemmet (161072), the Swedish Society of Medicine (SLS-595621, both to Dr. Halle) and the Stockholm County Council (SLL20170080 to Drs. Halle and Hansson) and funding from the Swedish Heart-Lung-Foundation (20120615, 20130664, 20140186),

ISSN 2452-302X https://doi.org/10.1016/j.jacbts.2018.10.006

SUMMARY

As a consequence of the success of present-day cancer treatment, radiotherapy-induced vascular disease is emerging. This disease is caused by chronic inflammatory activation and is likely orchestrated in part by microRNAs. In irradiated versus nonirradiated conduit arteries from patients receiving microvascular free tissue transfer reconstructions, irradiation resulted in down-regulation of miR-29b and up-regulation of miR-146b. miR-29b affected inflammation and adverse wound healing through its targets pentraxin-3 and dipeptidyl-peptidase 4. In vitro and in vivo, we showed that miR-29b overexpression therapy, through inhibition of pentraxin-3 and dipeptidyl-peptidase 4, could dampen the vascular inflammatory response.

ABBREVIATIONS AND ACRONYMS

$Apoe^{-/-}$ = apolipoprotein E knockout

DIG = digoxigenin

DPP4 = *Dpp4*, dipeptidyl-peptidase 4

FFT = free flap tissue transfer

HCtAEC = human carotid artery endothelial cell

HCtASMC = human carotid artery smooth muscle cell

mRNA = messenger ribonucleic acid

miRNA = microRNA

NR = nonirradiated

PTX3 = *Ptx3*, pentraxin-3

RNA = ribonucleic acid

SMC = smooth muscle cell

TGF = tumor growth factor

vRTx = radiation vasculopathy

Extraordinary efforts and great successes in cancer therapy have led to a growing cohort of cancer survivors (1). Despite being cancer-free, these patients have an increased risk of developing disease, ranging from cognitive impairment to heart failure, which can be attributed to previous cancer treatment (2). In this context, radiation-induced vascular disease or radiation vasculopathy (vRTx) is an under-recognized problem with high-impact long-term sequelae, such as stroke and myocardial infarction (3–5). In a manner proportional to radiation dosage and location, radiation therapy for breast cancer and Hodgkin lymphoma increases the risk for ischemic heart disease (6,7). In patients with head and neck cancer, carotid artery irradiation is a significant risk factor for carotid occlusive disease (5,8,9). In free flap tissue transfer (FFT) surgery, a procedure involving transplantation of a vascularized tissue by using microvascular anastomosis to repair large defects after tumor resection, irradiation is reported to be a risk factor for vascular complications (10–12).

The underlying pathophysiological mechanism of vRTx is a chronic inflammatory reaction initiated by the cellular response to ionizing radiation (13). In the vessel wall, this action induces various maladaptive events, including unbridled vascular cell proliferation, remodeling, and oxidative stress as well as tumor growth factor (TGF)-β-regulated nuclear factor kappa B activation. This type of chronic inflammatory reaction is known to cause intimal hyperplasia and accelerated atherosclerotic plaque development (14), leading to cardiovascular morbidity and mortality as well as reconstruction complications with FFT (15) in these patients.

Different cellular processes initiating the pathological vascular response are difficult to influence separately. MicroRNAs (miRNAs) have generated a great deal of attention because of their ability to critically regulate biological pathways (16). miRNAs can inhibit gene expression at different levels by acting as master regulators of protein output (17). miRNA modulation can influence and reverse disease processes and is used in preclinical as well as clinical studies (18,19). The vasculature, a sensitive and tightly regulated system, is especially under miRNA control, with it being implicated and applied in various vascular diseases (20,21). Moreover, miRNAs play a crucial role in the DNA damage response (22).

The current study investigated mechanisms through which down-regulation of miRNAs is involved in the adverse vascular response to irradiation and explored application of miRNA modulators as a therapeutic modality to reduce vRTx through dampening of the innate immune response and inhibition of an adverse healing response.

METHODS

HUMAN TISSUE SPECIMENS. Samples from Karolinska University Hospital's Biobank of Irradiated Tissues at Karolinska (Stockholm, Sweden) were

the Ragnar Söderberg Foundation (M-14/55), a DZHK Junior Research Group grant, a European Research Council Starting Grant (*NORVAS*), the Karolinska Institute Cardiovascular Program Career Development Grant, and the Swedish Research Council (2015-03140_4) (all to Dr. Maegdefessel). The authors have reported that they have no relationships relevant to the contents of this paper to disclose.

All authors attest they are in compliance with human studies committees and animal welfare regulations of the authors' institutions and Food and Drug Administration guidelines, including patient consent where appropriate. For more information, visit the *JACC: Basic to Translational Science* author instructions page.

Manuscript received August 15, 2018; revised manuscript received October 18, 2018, accepted October 18, 2018.

TABLE 1 Patient Characteristics

Age (yrs)/ Sex	RT Dose (Gy)	Time After Radiotherapy (weeks)	Donor Artery Origin	Current Smoking	CVD	NSAID Use
77/F	50	200	Forearm	No	No	No
64/M	68	44	Forearm	Yes	Yes	Yes
53/F	64	176	Fibula	Yes	No	Yes
45/F	64	119	Fibula	No	No	Yes
61/F	68	126	Fibula	No	No	Yes
79/M	64	620	Fibula	No	Yes	Yes
66/M	46	350	Fibula	No	No	Yes
52/M	68	100	Fibula	No	No	Yes
60/F	68	217	Fibula	No	No	No
60/M	46	50	Forearm	No	No	No
65/F	68	79	Forearm	No	No	Yes
70/M	66	128	Fibula	No	No	Yes
66/M	68	126	Thigh	No	No	No
39/F	68	83	Forearm	No	No	Yes
62/M	64	406	Fibula	No	No	No

CVD = cardiovascular disease; NSAID = nonsteroidal anti-inflammatory drug.

analyzed. Fifteen pairs of arterial biopsy samples were harvested during head and neck cancer reconstruction with microvascular free tissue transfer in 15 pre-operatively irradiated patients. Before performing microvascular anastomosis, biopsy samples were harvested from radiated branches of the external carotid artery (recipient site) and from the nonradiated (donor) artery of the transferred autologous tissue (Table 1). Biopsy samples were freed from surrounding tissue and surgical material under a dissection microscope, where care was taken not to damage the endothelium. Vascular tissue was placed in RNAlater (Thermo Fisher Scientific, Waltham, Massachusetts) or Allprotect Tissue Reagent (Qiagen, Hilden, Germany), frozen and stored at -80°C until ribonucleic acid (RNA) extraction. For immunohistochemical analysis, tissue from a paired subset of 3 patients was fixed in 10% formalin and paraffin embedded.

The study was approved by the Ethical Committee of Stockholm and was performed in agreement with institutional guidelines and the principles of the Declaration of Helsinki. All enrolled patients gave written, informed consent.

IN VITRO EXPERIMENTS. Cell culturing. Primary, proliferating human carotid artery smooth muscle cells (HCtASMCs) and human carotid artery endothelial cells (HCtAECs) (Cell Applications, San Diego, California) were cultured up to passages 5 through 8 in subtype-specific growth medium (Cell Applications). Cells were seeded on 6-, 12-, or 24-well plates and treated or radiated at a density of 70% to 80%. Endothelial cells were cultured and seeded in gelatin-coated (Attachment Factor Protein 1X, Thermo Fisher Scientific) flasks and plates.

Luciferase reporter assay. Luciferase reporter assay was performed as previously described (23). In brief, HEK293 cells (Public Health England Culture Collections, Salisbury, United Kingdom) were seeded on 96-well (PTX3, 1×10^4 cells/well) and 24-well (1×10^5 cells/well) plates. At 50% to 60% confluence, cells were transfected with luciferase reporter plasmid pLS, pLS-*DPP4*-3′UTR, or its mutant (100 ng/well, Active Motif), together with control or pre-miR-29b (10 nmol/l final concentration) by using DharmaFECT DUO Transfection Reagent (Thermo Fisher Scientific) according to the manufacturer's protocol. After a 24-h transfection period, luciferase activity was quantified by using the LightSwitch Luciferase Assay Kit (Thermo Fisher Scientific) according to the manufacturer's instructions.

Irradiation. Cells were placed inside a biological irradiator and were treated with 2 doses of 2 Gy (0.4 Gy/min; total irradiation time, 2 × 5 min) with 24 h between radiation dosages. Control cells were taken out of the incubator for a similar amount of time but did not receive irradiation.

KINETIC LIVE CELL IMAGING FOR PROLIFERATION AND APOPTOSIS. Cells in 6-well (for protein analysis) or 24-well (for RNA analysis) plates were used for these experiments. Directly after irradiation, medium was removed and replaced with fresh medium (Cell Applications). Cells were placed in a live-cell imaging incubator (IncuCyte, Essen Bioscience, Hertfordshire, United Kingdom) and images taken every 2 h for the course of 5 days. Proliferation was defined as an increase in cell confluence as the average of 9 pictures per well in a 24-well plate or 16 pictures per well in a 6-well plate. For apoptosis measurements, cell medium was supplied with caspase-3/7 reagent (Essen Bioscience) at a concentration of 5 μmol/l, as recommended by the manufacturer. Apoptosis was measured as the number of positive cells per photographed area. Experiments were run in triplicate.

IN VIVO IRRADIATION. In vivo experiments were approved by the Swedish Board for Agriculture (ethical permit no. N89/13). For in vivo irradiation, we used 10-week-old C57BL6/N apolipoprotein E knockout (*Apoe*$^{-/-}$) mice (Taconic Biosciences, Rensselaer, New York) weighing 20 to 30 g. Anesthesia consisted of intraperitoneal injection of 750 μg ketamine (Ketalar, Pfizer, Sollentuna, Sweden), 10 μl (1 mg/ml) of medetomidine (Domitor, Orion Pharma

Animal Heath, Sollentuna, Sweden), and 75 μl of phosphate-buffered saline. Depth of anesthesia was verified with a pedal reflex test. Animals (n = 9 to 11 per group) were fixated onto a heating pad and covered by a 7-mm-thick lead chamber with an open area (1.5 × 2.2 cm) also restricted by a collimator (2.5 × 2 cm) exposing the upper chest and neck region to radiation beams. Mice were placed in a biological irradiator (X-RAD 320, Precision X-Ray Inc., North Branford, Connecticut), and the uncovered area was irradiated at 0.7 Gy/min to a total dose of 14 Gy at 320 kV, 12.5 mA, 8 FOS, with an F2 filter consisting of aluminum, copper, and tin. Control mice received sham irradiation.

After irradiation, mice received atipamezole (Antisedan, Orion Pharma Animal Heath) 20 μl (5 mg/ml) for anesthesia reversal. Harvesting and organ handling are described in the Supplemental Methods section.

IN VIVO miR-29B MODULATION. For miR-29b overexpression, radiated mice (n = 6) received 2 dosages of 2 mg/kg miR-29b mimics (Ambion, Thermo Fisher Scientific) using the vector reagent Jet-PEI (Polyplus-transfection SA, Illkirch-Graffenstaden, France) for transfection. Control mice (n = 6) received 0.5 mg/kg (dosage according to the manufacturer's instructions) Jet-PEI–carried mimics with random (scrambled) sequences (Thermo Fisher Scientific). Mimics and controls were injected intraperitoneally 1 day before and 1 day after irradiation. Tissues were harvested 14 days after irradiation.

PREPARATION OF CELLS AND TISSUE SAMPLES FOR QUANTITATIVE REVERSE TRANSCRIPTION-POLYMERASE CHAIN REACTION. RNA isolation was performed according to standardized procedures described in the Supplemental Methods section. miRNA and messenger ribonucleic acid (mRNA) expression was quantified according to quantitative polymerase chain reaction using TaqMan (Thermo Fisher Scientific) FAM- or VIC-labeled mRNA and miRNA assays (Supplemental Tables 1 to 3).

TISSUE HISTOLOGY. Human tissue was fixed for 48 h in 10% formalin at room temperature, paraffin embedded, and cut into 5-μm-thick slides. Hematoxylin and eosin, Oil Red O, Sirius Red, and immunohistochemical stainings were performed according to standardized protocols. All primary antibodies were purchased from Abcam, Cambridge, United Kingdom (Supplemental Table 4). Dipeptidyl-peptidase 4 (DPP4)- and pentraxin-3 (PTX3)-positive cells were measured by counting the cells in 4 high-power fields of 2 to 4 different (human or mouse) vessels per group (nonradiated vs. irradiated in human; miR-29b modulated in mice upon radiation or sham irradiation). Counting was performed by a blinded investigator using ImageJ software (National Institutes of Health, Bethesda, Maryland). All histological analyses were obtained at room temperature by using a Hamamatsu NanoZoomer Slide Scanner with NDP.view2 software (Hamamatsu Photonics, Hamamatsu, Japan). More details are provided in the Supplemental Methods section.

IN SITU HYBRIDIZATION. For in situ hybridization, we used Exiqon miRCURY locked nucleic acid double digoxigenin (DIG)-labeled probes (50-30 probe sequence for miR-29b, AACACTGATTTCAAATGGT GCT; miR-146b, AGCCTATGGAATTCAGTTCTCA) with the accompanying kit and protocol (Qiagen, Hilden, Germany). In brief, tissue sections were deparaffinized. Nucleases were inactivated with proteinase K followed by a 2-h hybridization at hybridization temperature (53°C). Slides were washed in saline sodium citrate buffers. DIG-labeled probes were detected by using standard DIG detection methods.

STATISTICAL METHODS. SPSS version 22 (IBM Corporation, Armonk, New York) was used to analyze patient data. To compare 2 groups, Student's *t*-test was used. Paired data were analyzed by using paired-sample *t*-tests. Differences between ≥2 groups versus a control group were analyzed with 1-way analysis of variance plus a Bonferroni correction for multiple comparisons. Statistical analysis for the murine experimental data was conducted by using GraphPad Prism software version 7.0 (GraphPad Software, La Jolla, California). Differences in RNA expression were calculated as fold change versus control by using the mean delta Ct ($^{\Delta}$Ct, defined as $Ct^{\text{target RNA}}$ minus $Ct^{\text{endogenous control}}$) within groups. To correct for multiple *t*-tests in the live cell imaging experiments, the Holm-Šidák method with an alpha of 0.05 was used.

RESULTS

miR-29B IS DECREASED AND miR-146B INCREASED IN RADIATED VERSUS NONRADIATED VASCULAR TISSUE. In 15 pairs of arterial tissue samples from 15 patients undergoing microvascular free tissue transfer reconstructions (FFT), we compared the expression of 11 well-known miRNAs in cardiovascular disease, cancer, or both (Supplemental Table 1, **Figure 1A**). For some tissue pairs, miRNA expression could not be measured because of insufficient total RNA quantity (**Figure 1B**). Patient age ranged from 39 to 79 years (median, 62 years). Total radiation dosage

FIGURE 1 miRNA and Target Profiling in Radiated Versus Nonradiated Human Arteries

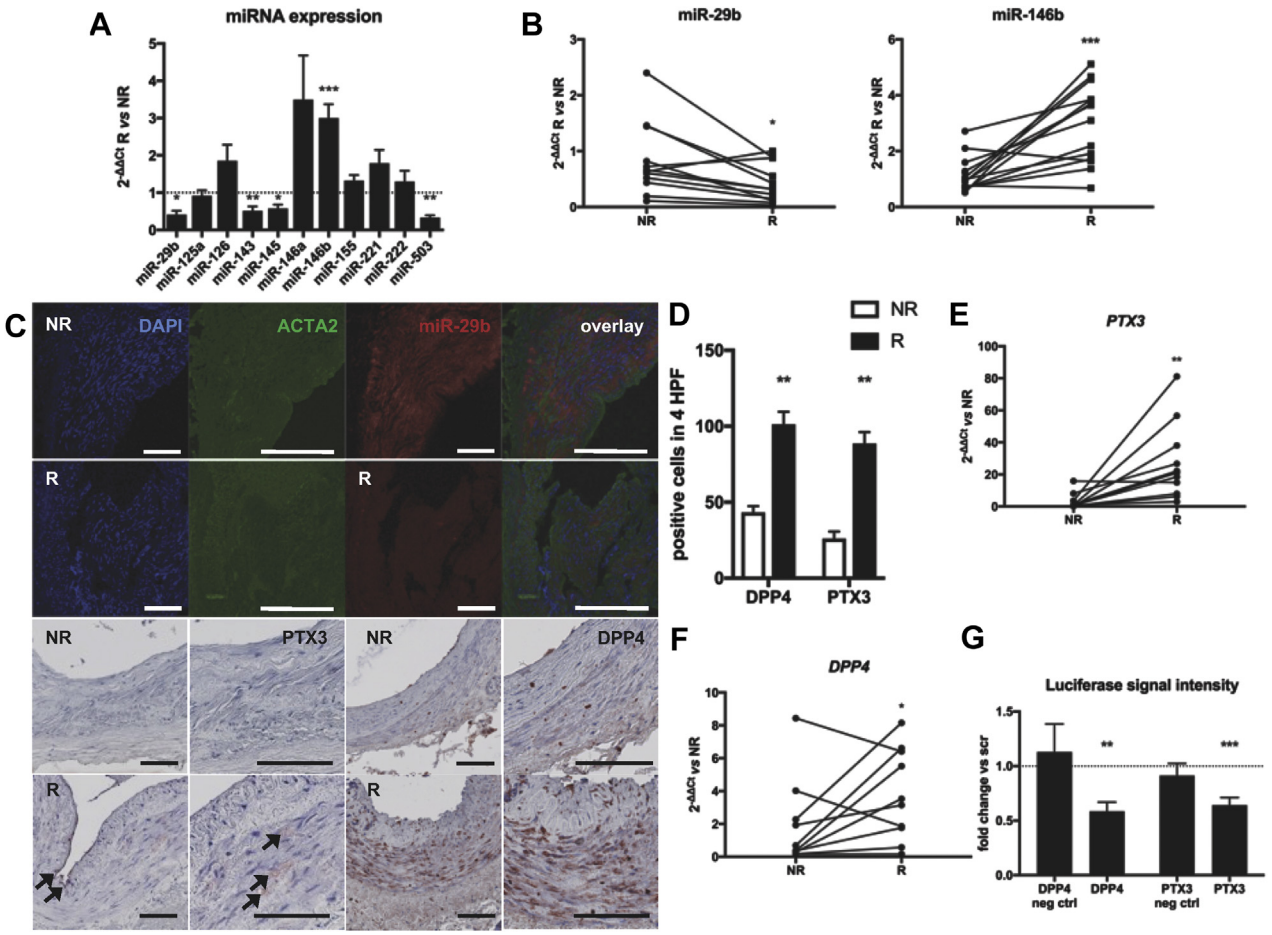

(A) Expression of 11 vascular disease-related microRNAs (miRNAs) in radiated (R) versus nonradiated (NR) arteries. n = 12 per group. Mean ± SEM. *p < 0.05; **p < 0.01; ***p < 0.001. **(B)** miR-29b was down-regulated and miR-146b upregulated in radiated versus nonradiated arteries harvested at microvascular tissue transfers. n = 15. *p < 0.05; ***p < 0.001. **(C)** Fluorescent in situ hybridization of miR-29b showing its expression in the tunica media of nonradiated vessels. Pentraxin-3 (PTX3) and dipeptidyl-peptidase 4 (DPP4) protein expression is increased throughout the vessel wall after radiation. ACTA2 = smooth muscle actin; DAPI = 4′,6-diamidino-2-phenylindole. Bars, 100 μm. **(D)** Quantification of staining for miR-29b target protein markers. n = 3 in each group. HPF = high-power field. **p < 0.01 in 1-way analysis of variance. **(E)** miR-29b target *PTX3* was up-regulated after irradiation. n = 10. **p < 0.01. **(F)** miR-29b target *DPP4* was upregulated after irradiation. n = 10. *p < 0.05, **p < 0.01, ***p < 0.001 in paired-sample *t*-tests. **(G)** miR-29b mimics significantly inhibited *DPP4* and *PTX3* luciferase activity compared with scrambled control (scr) oligonucleotides. Mean ± SEM. **p < 0.01, ***p < 0.001 in Student's *t*-test of scrambled versus miR-29b mimic. *EV* = empty vector; *mut* = mutated seed sequence; Neg ctrl = negative control.

was between 46 and 68 Gy (median, 66 Gy). Tissue was harvested during FFT, which occurred between 44 and 620 weeks after radiotherapy (median, 126 weeks). Other patient characteristics are listed in Table 1.

Among other miRNAs, miR-29b and miR-146b were significantly deregulated in radiated tissue, miR-29b being decreased and miR-146b increased (Figure 1B). Fluorescent in situ hybridization of miR-29b in these arteries was concordant with quantitative reverse transcription-polymerase chain reaction results, both miRNAs having a clear predilection for the intimal-medial layer, where smooth muscle cells (SMCs) reside (Figures 1C and 1D, top 2 rows). miR-143-145 and miR-503 were down-regulated along with miR-29b (Figure 1A). These 2 miRNAs were not further investigated because they could not be detected in human SMCs or endothelial cells in vitro (miR-503) or because of their mRNA target profile was more associated with SMC development and phenotype than with innate immunity (miR-143-145 cluster).

FIGURE 2 Murine Vascular miR-29b, miR-146b, *Ptx3*, and *Dpp4* Expression After Irradiation

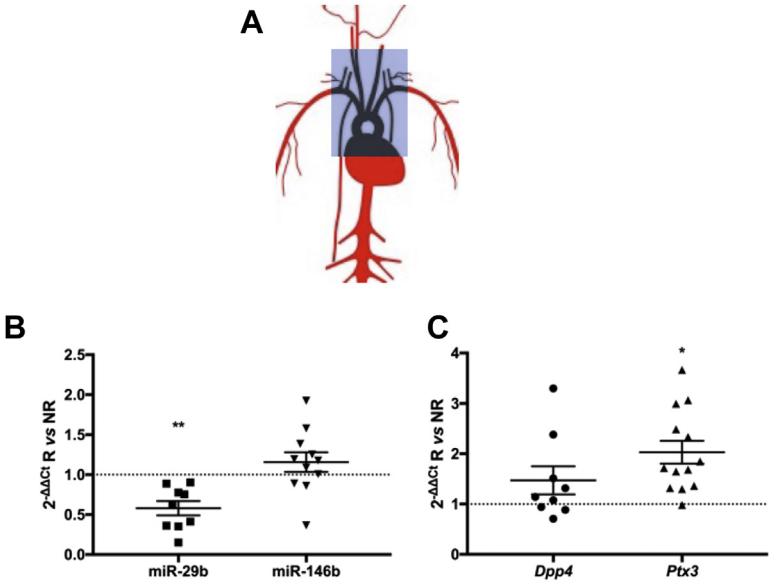

(A) Descriptive figure of the irradiated area in our in vivo radiation model. **(B)** Expression of miR-29b, but not of miR-146b, was altered in irradiated arterial tissue. n = 9 to 11 in each group. **(C)** Irradiation caused up-regulation of *Ptx3* gene expression but not *Dpp4* gene expression. Mean ± SEM. *$p < 0.05$; **$p < 0.01$ in Student's *t*-test. Abbreviations as in Figure 1.

EXPRESSION OF miR-29B TARGETS PTX3 AND DPP4 IS INCREASED UPON IRRADIATION. In previously published RNA analyses with the same method used in different samples, with a more recent harvest after irradiation (13,24), we searched for experimentally validated (25) miR-29b and miR-146b gene targets regulated in a direction inverse to that of the miRNA. In radiated versus nonradiated tissue, PTX3 was the most profoundly upregulated miR-29b target (Figure 1E). DPP4 levels were also significantly higher in radiated tissue (Figure 1F). The predicted miR-29b gene target DPP4 (or CD26) is related to radiation injury and impaired wound healing (26). With luciferase reporter assay, PTX3 and DPP4 were validated as miR-29b targets in HEK293 cells (Figure 1G).

In formalin-fixed, paraffin-embedded arterial tissue from a subset of patients, we could localize PTX3 and DPP4 protein expression in the intimal and medial layer of radiated arteries, whereas expression in their nonradiated counterparts was markedly lower (Figures 1C [bottom two rows] and 1D).

IRRADIATION AFFECTS VASCULAR miR-29B AND *PTX3* EXPRESSION IN A MURINE MODEL. Male *Apoe*$^{-/-}$ mice were subjected to irradiation using a model based on the method described by Stewart et al. (27). In mice receiving a single irradiation dose of 14 Gy in a designated mediastinal and neck area, including the heart and large vessels (Figure 2A), irradiated arteries exhibited a significant down-regulation of miR-29b and no significant up-regulation of miR-146b at 14 days compared with those given sham irradiation (Figure 2B). There was significant concordant up-regulation of Ptx3 after irradiation. *Dpp4* gene expression showed a trend toward up-regulation but was not significantly affected (Figure 2C). Histological analysis of the carotid artery 10 weeks after irradiation revealed no striking fibrotic or atherosclerotic differences between the radiated and sham radiated mice (Supplemental Figure 1).

miR-29B AND miR-146B EXPRESSION LEVELS, AND THEIR TARGETS, REACT TO IRRADIATION IN VITRO. Using a biological irradiator, we exposed human carotid artery SMCs and endothelial cells (HCtASMCs and HCtAECs) to 2 consecutive irradiation (radiotherapy) doses of 2 Gy, with 24 h between radiotherapy fractions, which was determined by the common clinical radiotherapy regimen for head and neck tumors (28). Radiotherapy significantly inhibited HCtASMC proliferation, which was statistically significant from 4 days after the last exposure (Supplemental Figures 2A and 2B). HCtAEC proliferation was not significantly affected (Supplemental Figure 2C). We measured miRNA and target gene expression 24 h after radiotherapy. In radiated

FIGURE 3 Irradiation Affects miR-29b, miR-146b, and Target Gene Expression In Vitro; Pathological Changes Are Partly Corrigible With miRNA Mimics

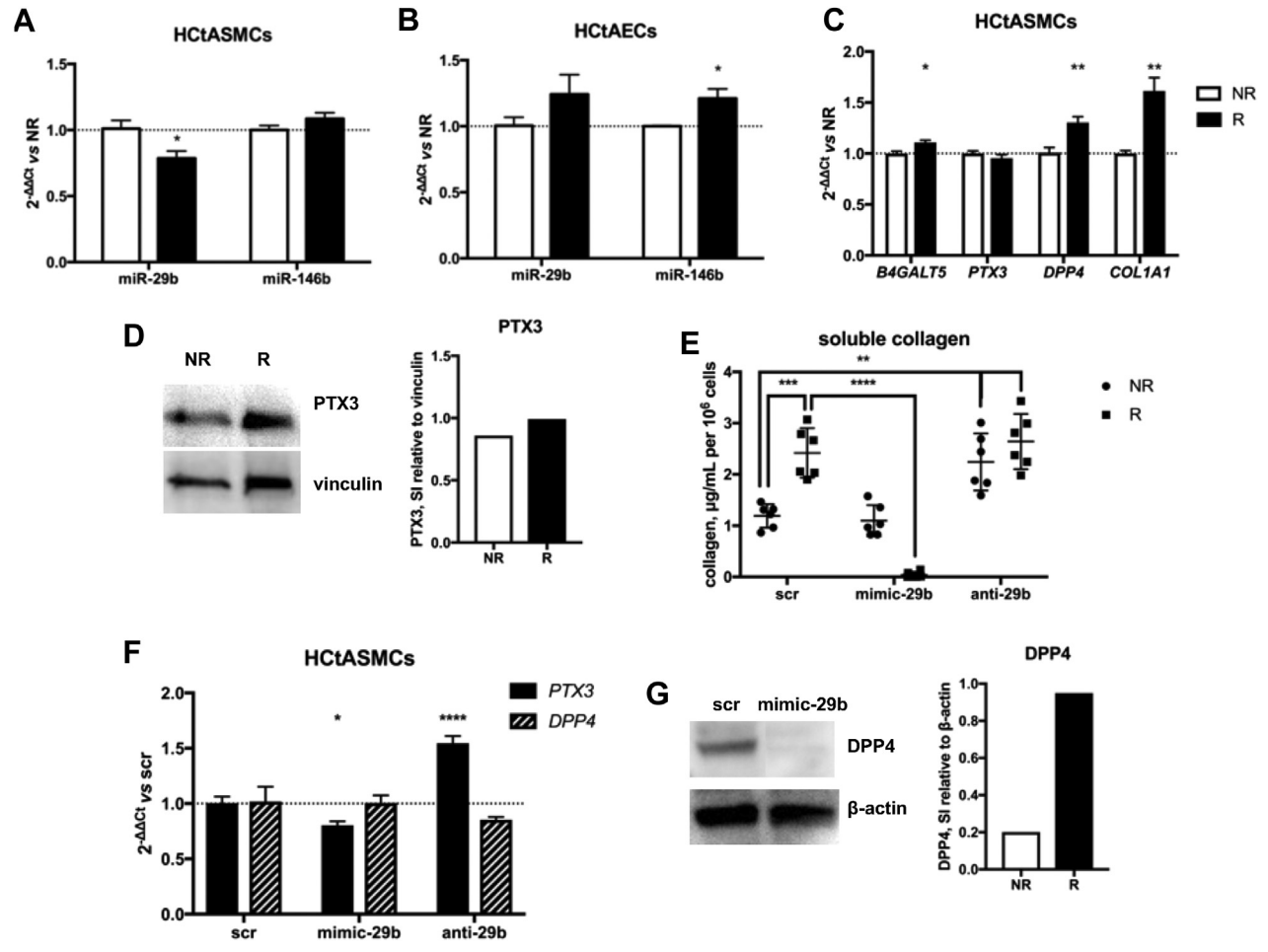

(A) In human carotid artery smooth muscle cells (HCtASMCs), 2 × 2 Gy of irradiation resulted in significantly reduced miR-29b expression; miR-146b expression was not affected. *p < 0.05. **(B)** The opposite was observed with human carotid artery endothelial cells (HCtAECs). *p < 0.05. **(C)** miR-29b target gene expression in HCtASMCs after irradiation. n = 6 in each group. Mean ± SEM. *p < 0.05, **p < 0.01 in Student's *t*-test. **(D)** Western blot analysis showed an increase in PTX3 protein expression after irradiation. **(E)** Treatment with miR-29b mimics resulted in undetectable soluble collagen in supernatant from radiated HCtASMCs but not from control HCtASMCs. **p < 0.01; ***p < 0.001; ****p < 0.0001. **(F)** miR-29b mimic treatment reduced *PTX3* expression in HCtASMCs. n = 6 in each group. Mean ± SEM. *p < 0.05, ****p < 0.0001 in 1-way analysis of variance. *DPP4* gene expression remained unchanged but was reduced on the protein level as shown with **(G)** Western blotting of HCtASMCs. Other abbreviations as in Figure 1.

HCtASMCs, but not in HCtAECs, miR-29b was down-regulated (Figure 3A). Radiated HCtAECs, but not HCtASMCs, exhibited up-regulation of miR-146b (Figure 3B). In HCtASMCs, expression of the miR-29b targets B4GALT5, DPP4, and COL1A1 was increased (Figure 3C). Although *PTX3* gene expression was not increased, Western blotting showed elevated levels of PTX3 protein in these cells (Figure 3D).

miR-29b is known to regulate extracellular matrix function by targeting collagen genes (29). Gamma radiation is well known to cause a TGF-β–mediated fibrotic response induced by fibroblasts (30) and SMCs (31). In radiated cells, a nonsignificant upward trend was observed in soluble collagen secretion, as measured in supernatant sampled 24 h after radiotherapy (Supplemental Figure 2D).

MODULATION OF miR-29B ALTERS EXPRESSION OF INFLAMMATION- AND FIBROSIS-RELATED TARGETS IN VITRO. Transfection of HCtASMCs with miR-29b mimics before radiotherapy completely abrogated soluble collagen secretion (Figure 3E) and decreased post-radiotherapy *PTX3* expression, whereas anti-miR-29b greatly stimulated *PTX3* expression

FIGURE 4 miR-29b Mimics Dampen Acute vRTx

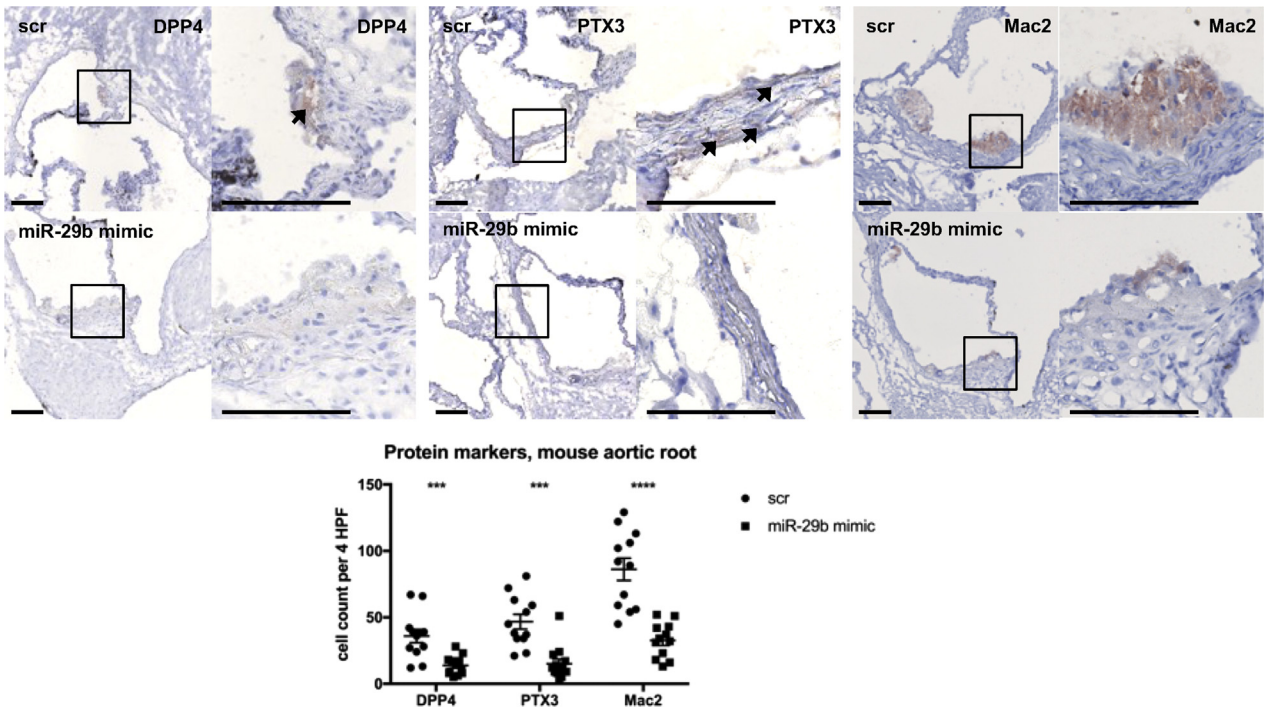

Jet-PEI–delivered miR-29b mimics caused decreased DPP4 protein expression in aortic root plaque, as well as a reduction in PTX3 protein in the vessel wall. Staining for the macrophage surface glycoprotein galectin-3 (Mac-2) revealed significantly increased macrophage influx in scrambled- compared with mimic-treated mice. Bars, 200 μm. n = 12 in each group. Mean ± SEM. ***p < 0.001, ****p < 0.0001 in 1-way analysis of variance. vRTx = radiation vasculopathy; other abbreviations as in Figure 1.

(Figure 3F). Interestingly, anti-miR-29b had no marked profibrotic effect in radiated cells, possibly because further suppression of already low miR-29b levels does not add to the fibrotic stimulus. In nonradiated cells, however, it induced a significant increase in soluble collagen production. Profibrotic DPP4 was not affected by miR-29b on the gene expression level, but Western blotting in HCtASMC lysates showed that expression of DPP4 protein was negatively affected by transfection with miR-29b mimics (Figure 3G). Because DPP4 has a soluble form, detectable in blood plasma and associated with a profibrotic phenotype, we assessed DPP4 expression in the supernatant of ECs or SMCs but could not detect the protein, independent of irradiation (data not shown).

MODULATION OF miR-29B AFFECTS TARGET PROTEIN EXPRESSION AND INFLAMMATION IN VIVO. We subjected 12 *Apoe*$^{-/-}$ male mice to the 1 × 14 Gy irradiation protocol, of which 6 received miR-29b mimics 1 day before and 1 day after irradiation. Target genes *Ptx3* and *Dpp4* were not significantly affected (Supplemental Figure 3A), but on the protein level, PTX3 and DPP4 expression showed marked differences in the medial layer of aortic ring tissue in scrambled- versus mimic-treated mice (Figure 4, left 2 panels). Staining for the macrophage surface glycoprotein galectin 3 (Mac-2) revealed marked macrophage influx in aortic ring atherosclerotic plaques of scrambled- compared with miR-29b mimic-treated mice (Figure 4, right panel). Smooth muscle actin staining revealed no differences in SMC quantity between miR-29b mimic-treated and control mice (Supplemental Figure 3B). Collectively, miR-29b mimics dampened the direct inflammatory reaction to irradiation, without affecting SMC content.

DISCUSSION

Irradiation is an important risk factor for atherosclerosis and subsequent cardiovascular disease (32,33). As master regulators in many cellular processes initiated by vascular injury, miRNAs can be crucial actors in vRTx. miRNAs play a crucial role in the DNA damage

response (22), and miRNA inhibition or stimulation can blunt irradiation effects on cell survival and proliferation (34). We have identified 2 miRNAs known to play a crucial role in vascular cell biology and pathology in relation to atherosclerosis, miR-29b and miR-146b, to be down- respectively up-regulated in irradiated vascular tissue. The expression of 2 well-known vascular miRNAs, miR-143 and miR-145, was also altered, but they were not further investigated; we consider that down-regulation of the atheroprotective miR-143-145 cluster as confirmation that irradiation induces an atheroprone phenotype.

miR-146a and miR-146b arise from 2 evolutionarily conserved miRNA genes located on chromosomes 5 and 10, respectively. In their mature form, they differ only by 2 nucleotides in the 3′ end. miR-146b, unlike miR-146a, is responsive to interleukin-10 and therefore might be involved in inflammation resolution (35). Enforced miR-146b expression in monocytes reduces production of a multitude of inflammatory cytokines (35,36), suggesting that this miRNA is part of a negative feedback loop limiting inflammation (37). We observed up-regulation of miR-146b in irradiated human arterial tissue. It is likely that this up-regulation is symptomatic of the chronic inflammatory response in vRTx and can be seen as an attempt to resolve inflammation. Inhibition of miR-146b would likely aggravate the inflammatory reaction and therefore be counterproductive; potentially beneficial effects of miR-146b mimics could be a direction for further investigation.

The miR-29 family of miRNAs consists of miR-29a and miR-29b-1, of which the encoding gene is located on chromosome 7, and miR-29b-2 and miR-29c, originating from chromosome 1. miR-29b-1 and miR-29b-2 have identical mature sequences, are therefore indistinguishable on polymerase chain reaction, and share the name miR-29b. In a vascular biological context, miR-29b is best known as regulator of the collagen- and extracellular matrix–associated mRNAs critically involved in cardiovascular fibrosis (38). miR-29b limits collagen gene expression and thus can weaken the vascular wall in abdominal aortic aneurysms (39), as well as the matrix of fibrous caps in atherosclerosis (40). Strategies of inhibiting miR-29b are thus an attractive option for increasing vessel wall and lesion stability. In vRTx, conversely, excess collagen production and turnover is pathognomonic for the maladaptive healing response. Inhibition of collagen production through miR-29b stimulation might therefore put an end to the downward spiral of inflammation and fibrosis in vRTx.

DPP4 (also known as CD26) is a transmembrane glycoprotein with an extracellular domain binding to adenosine deaminase and matrix proteins such as fibronectin and collagen (41). The function of DPP4 in vascular disease is under intensive investigation because its inhibitor, alogliptin (a novel glucose-lowering agent in the treatment of type 2 diabetes mellitus), displays antiatherogenic effects in low-density lipoprotein receptor knockout (42) and *Apoe*$^{-/-}$ mice (43). In addition, DPP4/CD26 indicates a type of fibroblasts with an increased profibrotic potential responsible for wounding- and irradiation-induced skin fibrosis and scarring, as well as tumor growth, through activation of the serine protease fibroblast activation protein-α (26). DPP4 has previously been proposed as a target of miR-29b (44), an interaction we were able to confirm in the vRTx context.

PTX3 is a secreted pattern recognition molecule providing resistance against fungal, bacterial, and viral pathogens. Together with its family members C-reactive protein and serum amyloid P component, it initiates complement activation and phagocytosis. In contrast to C-reactive protein, PTX3 is evolutionarily well conserved (45) and expressed within the vasculature, making it a good target to study in humans as well as animal models within this context. Interestingly, PTX3 has inflammatory as well as regulatory capacities, as its release induces both proinflammatory and anti-inflammatory signaling (46,47). PTX3 is a validated target of miR-29b (48) and a key regulatory protein in pathophysiological processes in which innate immunity, inflammation, and extracellular matrix remodeling intersect (45).

In vRTx, we have previously described sustained high expression of *PTX3* mRNA at earlier time points after radiotherapy (24). The current study is the first to describe gene expression patterns in irradiated human arteries at a median of >2 years after radiotherapy. Tissue damage caused by radiation injury is commonly divided into early and late adverse effects, according to the time elapsed from treatment to symptoms. Early adverse effects typically affect rapidly proliferating cells, such as epithelial cells of the skin and mucosa, whereas late adverse effects often are an effect of a progressive, systemic disease in which symptoms may not be evident until decades after radiotherapy (49,50).

STUDY LIMITATIONS. vRTx is the result of a pathologic stimulus (irradiation), creating a cascade of inflammatory reactions. Depending on timing after irradiation, various maladaptive vascular changes can

be observed, and timing of (preventive) therapy appears crucial. This study proposes miR-29b overexpression as a potential preventive therapy, but could not identify an optimal administration time-point, which in part relates to the experimental murine model not completely being able to reflect all moieties of human radiotherapy-induced disease. The lack of an ideal in vivo model that is able to mimic the various features of human disease remains problematic for most cardiovascular diseases. Furthermore, other miRNAs and targets that were not assessed by us, might likely also play important roles in vRTx and could be modulated to prevent the disease. Their effects remain to be elucidated in further studies.

CONCLUSIONS

In vivo and in vitro, we showed that PTX3 and DPP4 expression are hallmarks of radiation injury to vascular tissues and can be suppressed with miR-29b mimics. These findings not only suggest that stimulation of miR-29b can be a candidate therapy to prevent vRTx but also stress the importance of a cautious approach when considering miR-29b inhibition as therapy against various atherosclerotic disease manifestations. In patients with vRTx associated with perivascular fibrosis (51), miR-29b stimulation, rather than inhibition, might be the most effective treatment.

ACKNOWLEDGMENTS The Swedish Radiation Safety Authority provides advice and information in the event of a nuclear energy accident as well as any other incident or accident involving radiation.

ADDRESS FOR CORRESPONDENCE: Dr. Lars Maegdefessel, Karolinska Institute, Department of Medicine, Solna, 171 76 Stockholm, Sweden. E-mail: lars.maegdefessel@ki.se.

PERSPECTIVES

COMPENTENCY IN MEDICAL KNOWLEDGE: Radiotherapy is an established and powerful therapeutic strategy for the treatment of patients with cancer. The downside for this form of curative approach is a substantial increase in cardiovascular complications. Thus, supportive treatment schemes need to be developed to limit the risk and burden of radiotherapy-induced vasculopathies. The targeting of miRNAs via antisense oligonucleotides could serve as a sufficient and effective approach to limit the multiple features (inflammation, fibrosis, and proliferation) associated with radiotherapy-induced vasculopathies.

TRANSLATIONAL OUTLOOK: Safety and efficiency of miRNA mimics are currently under investigation, and interestingly a Phase II clinical trial utilizing miR-29 mimics (promiR-29, Remlarsen) is ongoing in cutaneous fibrotic disorders. Here, mimics are being applied topically to the skin, which limits undesired off-target effects in organ systems in which systemically administered miRNA modulators assimilate to a much higher degree (e.g., liver, kidney). For the treatment of vascular diseases, cell type–specific or local ways of delivery (using stents and balloons) could limit off-target effects, while triggering local uptake and efficiency of these potent therapies.

REFERENCES

1. DeSantis CE, Lin CC, Mariotto AB, et al. Cancer treatment and survivorship statistics, 2014. CA Cancer J Clin 2014;64:252–71.

2. Shahrokni A, Wu AJ, Carter J, Lichtman SM. Long-term toxicity of cancer treatment in older patients. Clin Geriatr Med 2016;32:63–80.

3. Groarke JD, Nguyen PL, Nohria A, Ferrari R, Cheng S, Moslehi J. Cardiovascular complications of radiation therapy for thoracic malignancies: the role for non-invasive imaging for detection of cardiovascular disease. Eur Heart J 2014;35:612–23.

4. Jaworski C, Mariani JA, Wheeler G, Kaye DM. Cardiac complications of thoracic irradiation. J Am Coll Cardiol 2013;61:2319–28.

5. Plummer C, Henderson RD, O'Sullivan JD, Read SJ. Ischemic stroke and transient ischemic attack after head and neck radiotherapy: a review. Stroke 2011;42:2410–8.

6. Darby SC, Ewertz M, McGale P, et al. Risk of ischemic heart disease in women after radiotherapy for breast cancer. N Engl J Med 2013;368:987–98.

7. Nilsson G, Holmberg L, Garmo H, et al. Distribution of coronary artery stenosis after radiation for breast cancer. J Clin Oncol 2012;30:380–6.

8. Gujral DM, Chahal N, Senior R, Harrington KJ, Nutting CM. Radiation-induced carotid artery atherosclerosis. Radiother Oncol 2014;110:31–8.

9. Abayomi OK. Neck irradiation, carotid injury and its consequences. Oral Oncol 2004;40:872–8.

10. Fosnot J, Fischer JP, Smartt JM Jr., et al. Does previous chest wall irradiation increase vascular complications in free autologous breast reconstruction? Plast Reconstr Surg 2011;127:496–504.

11. Herle P, Shukla L, Morrison WA, Shayan R. Preoperative radiation and free flap outcomes for head and neck reconstruction: a systematic review and meta-analysis. ANZ J Surg 2015;85:121–7.

12. Halle M, Bodin I, Tornvall P, Wickman M, Farnebo F, Arnander C. Timing of radiotherapy in head and neck free flap reconstruction—a study of postoperative complications. J Plast Reconstr Aesthet Surg 2009;62:889–95.

13. Halle M, Gabrielsen A, Paulsson-Berne G, et al. Sustained inflammation due to nuclear factor-kappa B activation in irradiated human arteries. J Am Coll Cardiol 2010;55:1227–36.

14. Libby P, Ridker PM, Hansson GK. Progress and challenges in translating the biology of atherosclerosis. Nature 2011;473:317–25.

15. Tall J, Bjorklund TC, Skogh AC, Arnander C, Halle M. Vascular complications after radiotherapy in head and neck free flap reconstruction: clinical outcome related to vascular biology. Ann Plast Surg 2015;75:309–15.

16. Bartel DP. MicroRNAs: target recognition and regulatory functions. Cell 2009;136:215–33.

17. Ebert MS, Sharp PA. Roles for microRNAs in conferring robustness to biological processes. Cell 2012;149:515–24.

18. Gomez IG, MacKenna DA, Johnson BG, et al. Anti-microRNA-21 oligonucleotides prevent Alport nephropathy progression by stimulating metabolic pathways. J Clin Invest 2015;125:141–56.

19. Janssen HL, Reesink HW, Lawitz EJ, et al. Treatment of HCV infection by targeting microRNA. N Engl J Med 2013;368:1685–94.

20. Schober A, Nazari-Jahantigh M, Weber C. MicroRNA-mediated mechanisms of the cellular stress response in atherosclerosis. Nat Rev Cardiol 2015;12:361–74.

21. van Rooij E, Olson EN. MicroRNA therapeutics for cardiovascular disease: opportunities and obstacles. Nat Rev Drug Discov 2012;11:860–72.

22. Wan G, Mathur R, Hu X, Zhang X, Lu X. miRNA response to DNA damage. Trends Biochem Sci 2011;36:478–84.

23. Li Y, Challagundla KB, Sun XX, Zhang Q, Dai MS. MicroRNA-130a associates with ribosomal protein L11 to suppress c-Myc expression in response to UV irradiation. Oncotarget 2015;6:1101–14.

24. Christersdottir Bjorklund T, Reilly SJ, Gahm C, et al. Increased long-term expression of pentraxin 3 in irradiated human arteries and veins compared to internal controls from free tissue transfers. J Translat Med 2013;11:223.

25. Hsu SD, Lin FM, Wu WY, et al. miRTarBase: a database curates experimentally validated microRNA-target interactions. Nucleic Acids Res 2011;39:D163–9.

26. Rinkevich Y, Walmsley GG, Hu MS, et al. Skin fibrosis. Identification and isolation of a dermal lineage with intrinsic fibrogenic potential. Science 2015;348:aaa2151.

27. Stewart FA, Heeneman S, Te Poele J, et al. Ionizing radiation accelerates the development of atherosclerotic lesions in ApoE-/- mice and predisposes to an inflammatory plaque phenotype prone to hemorrhage. Am J Pathol 2006;168:649–58.

28. Bartelink H, Van den Bogaert W, Horiot JC, Jager J, van Glabbeke M. Concomitant cisplatin and radiotherapy in a conventional and modified fractionation schedule in locally advanced head and neck cancer: a randomised phase II EORTC trial. Eur J Cancer 2002;38:667–73.

29. Kriegel AJ, Liu Y, Fang Y, Ding X, Liang M. The miR-29 family: genomics, cell biology, and relevance to renal and cardiovascular injury. Physiol Genomics 2012;44:237–44.

30. Burger A, Loffler H, Bamberg M, Rodemann HP. Molecular and cellular basis of radiation fibrosis. Int J Radiat Biol 1998;73:401–8.

31. Alexakis C, Guettoufi A, Mestries P, et al. Heparan mimetic regulates collagen expression and TGF-beta1 distribution in gamma-irradiated human intestinal smooth muscle cells. FASEB J 2001;15:1546–54.

32. Gray K, Kumar S, Figg N, et al. Effects of DNA damage in smooth muscle cells in atherosclerosis. Circ Res 2015;116:816–26.

33. Bashar K, Healy D, Clarke-Moloney M, Burke P, Kavanagh E, Walsh SR. Effects of neck radiation therapy on extra-cranial carotid arteries atherosclerosis disease prevalence: systematic review and a meta-analysis. PLoS One 2014;9:e110389.

34. Wagner-Ecker M, Schwager C, Wirkner U, Abdollahi A, Huber PE. MicroRNA expression after ionizing radiation in human endothelial cells. Radiat Oncol 2010;5:25.

35. Curtale G, Mirolo M, Renzi TA, Rossato M, Bazzoni F, Locati M. Negative regulation of Toll-like receptor 4 signaling by IL-10-dependent microRNA-146b. Proc Natl Acad Sci U S A 2013;110:11499–504.

36. Hulsmans M, Van Dooren E, Mathieu C, Holvoet P. Decrease of miR-146b-5p in monocytes during obesity is associated with loss of the anti-inflammatory but not insulin signaling action of adiponectin. PLoS One 2012;7:e32794.

37. Cheng HS, Sivachandran N, Lau A, et al. MicroRNA-146 represses endothelial activation by inhibiting pro-inflammatory pathways. EMBO Mol Med 2013;5:949–66.

38. van Rooij E, Sutherland LB, Thatcher JE, et al. Dysregulation of microRNAs after myocardial infarction reveals a role of miR-29 in cardiac fibrosis. Proc Natl Acad Sci U S A 2008;105:13027–32.

39. Maegdefessel L, Azuma J, Toh R, et al. Inhibition of microRNA-29b reduces murine abdominal aortic aneurysm development. J Clin Invest 2012;122:497–506.

40. Ulrich V, Rotllan N, Araldi E, et al. Chronic miR-29 antagonism promotes favorable plaque remodeling in atherosclerotic mice. EMBO Mol Med 2016;8:643–53.

41. Zhong J, Maiseyeu A, Davis SN, Rajagopalan S. DPP4 in cardiometabolic disease: recent insights from the laboratory and clinical trials of DPP4 inhibition. Circ Res 2015;116:1491–504.

42. Akita K, Isoda K, Shimada K, Daida H. Dipeptidyl-peptidase-4 inhibitor, alogliptin, attenuates arterial inflammation and neointimal formation after injury in low-density lipoprotein (LDL) receptor-deficient mice. J Am Heart Assoc 2015;4:e001469.

43. Ta NN, Schuyler CA, Li Y, Lopes-Virella MF, Huang Y. DPP-4 (CD26) inhibitor alogliptin inhibits atherosclerosis in diabetic apolipoprotein E-deficient mice. J Cardiovasc Pharmacol 2011;58:157–66.

44. Shi S, Koya D, Kanasaki K. Dipeptidyl peptidase-4 and kidney fibrosis in diabetes. Fibrogenesis Tissue Repair 2016;9:1.

45. Mantovani A, Garlanda C, Doni A, Bottazzi B. Pentraxins in innate immunity: from C-reactive protein to the long pentraxin PTX3. J Clin Immunol 2008;28:1–13.

46. Bottazzi B, Doni A, Garlanda C, Mantovani A. An integrated view of humoral innate immunity: pentraxins as a paradigm. Annu Rev Immunol 2010;28:157–83.

47. Garlanda C, Jaillon S, Doni A, Bottazzi B, Mantovani A. PTX3, a humoral pattern recognition molecule at the interface between microbe and matrix recognition. Curr Opin Immunol 2016;38:39–44.

48. Abonnenc M, Nabeebaccus AA, Mayr U, et al. Extracellular matrix secretion by cardiac fibroblasts: role of microRNA-29b and microRNA-30c. Circ Res 2013;113:1138–47.

49. Stone HB, Coleman CN, Anscher MS, McBride WH. Effects of radiation on normal tissue: consequences and mechanisms. Lancet Oncol 2003;4:529–36.

50. Darby S, McGale P, Peto R, Granath F, Hall P, Ekbom A. Mortality from cardiovascular disease more than 10 years after radiotherapy for breast cancer: nationwide cohort study of 90 000 Swedish women. BMJ 2003;326:256–7.

51. Khan AA, Paget JT, McLaughlin M, Kyula JN, et al. Genetically modified lentiviruses that preserve microvascular function protect against late radiation damage in normal tissues. Sci Transl Med 2018;10(425).

KEY WORDS arteriosclerosis, inflammation, microRNA, radiotherapy

APPENDIX For an expanded Methods section as well as supplemental tables and figures, please see the online version of this paper.